TIME-STRATIGRAPHY AND IMPACT CRATERING CHRONOLOGY OF MERCURY. R. J. Wagner, U. Wolf, and G. Neukum. DLR, Institute of Space Sensor Technology and Planetary Exploration, Rutherfordstrasse 2, D-12489 Berlin, Germany (e-mail of corresponding author: Roland.Wagner@dlr.de)

Introduction: Mariner-10 was the only spacecraft which has visited the innermost planet Mercury so far in 1974/75. During three close encounters, the camera onboard Mariner-10 has acquired images of only about 40-45 % of the total surface at medium spatial resolutions between 1 and 4 km/pxl, with highest resolutions obtained in selected areas down to about 100 m/pxl. In this paper, we present results from (1) crater size-frequency measurements carried out on various geologic units, use (2) a recently updated crater production function polynomial, and (3) an updated impact cratering chronology model [1, and references therein] in order to reassess the time-stratigraphic system established for Mercury [2, 3, 4]. These investigations are prerequisite for further studies during two upcoming orbiting missions to Mercury, ESA's *Bepi-Colombo* and NASA's *Messenger*.

Geologic overview: Mercury exhibits a lunar-like surface, dominated by *impact craters* and *multi-ring basins* in various states of preservation [5, 6].

Geologic units: Three major geologic units were identified [7]: (a) *densely cratered terrain* (highlands), with (b) interspersed smooth areas, the so-called *inter-crater plains*, and (c) lightly cratered *low-land plains* (or *smooth plains*). Inter-crater plains in general embay older densely cratered highlands and degraded multi-ring structures [7]. Emplacement of inter-crater plains very likely caused crater obliteration in highland areas at crater diameters smaller than about 30 km, thus changing the shape of an otherwise ideal highland-type crater size-frequency distribution similar to the one found in lunar highland areas [8]. Low-land plains occur preferentially in association with impact structures, and in patches in highland areas [8]. They resemble lunar maria (except in brightness) and also feature wrinkle ridges [4]. Modes of emplacement for inter-crater plains and low-land plains are controversially discussed: some investigators favor an impact origin [7, 9], others conjecture a volcanic origin, despite the lack of unequivocal volcanic features [4, 5, 6].

Craters and multi-ring basins: Numerous basins with diameters larger than about 200 km and with at least two rings were found on Mercury [4]. Many of them are highly degraded and hence rather old features [10]. The *Caloris* basin is the youngest and largest one (about 1300 km in diameter) in the imaged part of the mercurian surface. Craters, similar in morphology to lunar craters, and, as these, with increasingly complex forms with increasing diameters, were subdivided into 5 erosional classes, ranging from fresh, bright ray craters (class C5) to heavily degraded crater ruins (C1) [3]. Some of the basins and craters provide important stratigraphic markers and were used to subdivide Mercury's geologic history into time-stratigraphic systems and chronologic periods [1, 2, 3, 4, 8].

Tectonic features: Mercury was tectonically active in the past. Lineaments with trends of NE-SW and NW-SE in the equatorial regions, and E-W in the polar regions, predate the younger multi-ring basins and are believed to have been created by tidal despinning [11, 12]. Thrusting events, caused by rapid cooling and contraction of Mercury, created scarps and scarp systems, such as *Discovery Rupes*, which extend over several hundred kilometers and which were formed before and after the Caloris event [11, 12].

Crater size-frequency measurements and impact cratering chronology: It has been discussed by several investigators that the shapes of crater size-frequency distributions measured on bodies in the inner solar system closely resemble each other, and also resemble the size distribution observed for Main Belt asteroids, which provide the major source of impactors on the terrestrial planets, with a contribution of comets being assumed to be much less than 10 % [1, 13, 14]. The lunar production function (a polynomial of 11^{th} degree), was refined recently and applied to Mercury, taking into account differences in crater scaling between the two bodies [1, 13, 14]. This polynomial is used to fit measured crater size-frequency distributions. Relative crater retention ages of geologic units are given as cumulative frequencies equal to, or greater than, a reference diameter of 10 km (*Tab. 1*). Estimates for Mercury/moon cratering rate ratios were used to derive a cratering chronology model function for Mercury [1, and references therein] (*Fig. 1*). It is characterized (a) by a rapid change in cumulative frequency with time for model ages older than about 3.3 Gyr (1 Gyr = 1 billion years), due to an exponential decay in cratering rate during the Late Heavy Bombardment (LHB) period, and (b) by only a small decrease in cumulative frequency with time for ages younger than about 3.3 Gyr, due to a more or less constant cratering rate ever since [1, 13]. Both cumulative frequencies for geologic units, based on the refined lunar production function, and their corresponding updated cratering model ages differ from values published earlier [8].

Time-stratigraphy of Mercury: Mercury's geologic history was subdivided into five time-

stratigraphic systems and chronologic periods [2, 3, 4]: (1) *pre-Tolstojan*, (2) *Tolstojan*, (3) *Calorian*, (4) *Mansurian*, and (5) *Kuiperian* (see *Fig. 1*).

Pre-Tolstojan: This period ranges from the formation of a crust until the formation of the Tolstoj multi-ring basin. Impacts created most of the highlands and a great number of now degraded multi-ring basins. Inter-crater plains were emplaced also in this period. Older highlands show a tectonic imprint of tidal despinning (lineaments). Toward the end of this period, planetary cooling and contraction started, creating scarps and scarp systems [4].

Tolstojan: The Tolstoj basin was created 3.97 Gyr ago, an age comparable to the 3.9 - 4 Gyr given by [4]. Smooth plains were emplaced, either by volcanism or impact. Tidal despinning and planetary contraction continued, causing lineaments and scarp systems to form [4].

Calorian: The impact of a large body, presumably an asteroid, created the Caloris basin about 3.77 Gyr ago. This age derived in our model is much less than the one given by [4] and is closer to the model age of the lunar Orientale basin. The Late Heavy Bombardment ends within this period.

Mansurian, Kuiperian: After the heavy bombardment, the cratering rate has been more or less constant until today. Younger craters were formed, superposing older units such as multi-ring basins and scarp systems [4]. Youngest formations on the mercurian surface are bright ray craters such as Kuiper (60 km diameter). As of now, this time-stratigraphic scheme is far from complete since only 40-45 % of Mercury's surface are known today, and since the spatial resolution of most parts of the surface imaged is not yet sufficient.

References: [1] Neukum G. et al., *Planet. Space Sci.* **49**, 1507 – 1521, 2001. [2] Holt H. E., in: *Repts. Planet. Geol. Prog.*, NASA *TM-79729* (abstract), 327, 1978. [3] McCauley J. F. et al., *Icarus 47*, 184-202, 1981. [4] Spudis P. D. and Guest J. E., in: *Mercury* (F. Vilas, C. R. Chapman, and M. S. Matthews, eds.), Univ. of Arizona Press, Tucson, 336-373, 1988. [5] Murray B. C. et al., *Science 185,* 169-179, 1974. [6] Murray B. C. et al., *JGR 80*, 2508-2514, 1975. [7] Trask N. J. and Guest J. E., *JGR 80*, 2462-2477, 1975. [8] Strom R. G. and Neukum G., in: *Mercury* (F. Vilas, C. R. Chapman, and M. S. Matthews, eds.), Univ. of Arizona Press, Tucson, 336-373, 1988. [9] Wilhelms D. E., *Icarus 28*, 551-558, 1976. [10] Pike R. J. and Spudis P. D., *Earth, Moon, and Planets* **39,** 129-194, 1987. [11] Melosh H. J. and McKinnon W. B., in: *Mercury* (F. Vilas, C. R. Chapman, and M. S. Matthews, eds.), Univ. of Arizona Press, Tucson, 374-400, 1988. [12] Thomas P. G. et al., in: *Mercury* (F. Vilas, C. R. Chapman, and M. S. Matthews, eds.), Univ. of Arizona Press, Tucson, 401-428, 1988. [13] Neukum G. et al., in: *Chronology and Evolution of Mars*, (W. K. Hartmann, J. Geiss, and R. Kallenbach, eds.), pp. 53 – 86, 2001. [14] Neukum G. and B. A. Ivanov, *Lunar Planet. Sci. Conf. XXXIII*, abstract #1263, 2002.

Geologic Unit	Cum. frequency (D>10 km)		Crat. model age (Gyr)	
	[8]	this work	[8]	this work
Kuiper	-	(4.04e-6)	-	(1.0)
Mansur	-	(2.31e-5)	-	(3.5)
Caloris	6.85e-5	7.51e-5	3.85	3.77±0.06
Beethoven	1.53e-4	1.22e-4	3.98	3.86±0.05
Tolstoj	2.65e-4	2.51e-4	4.06	3.97±0.05
Pushkin	3.45e-4	2.72e-4	4.10	3.98±0.06
Haydn	3.65e-4	2.76e-4	4.11	3.99±0.06
Dostojewskij	5.49e-4	2.75e-4	4.17	3.99±0.06
Chekhov	4.04e-4	4.15e-4	4.12	4.05±0.08
Highlands	5.99e-4	4.81e-4	4.18	4.07±0.03

Table 1: Cumulative frequencies (for D>10 km) and associated cratering model ages for major geologic units, craters and basins. Older values from [8] compared to updated values (this paper). Uncertainties for cumulative frequencies ([8], and this paper) are on the order of 20 - 30%, translating into model age uncertainties of 0.03 – 0.06 Gyr ([8], and this paper).

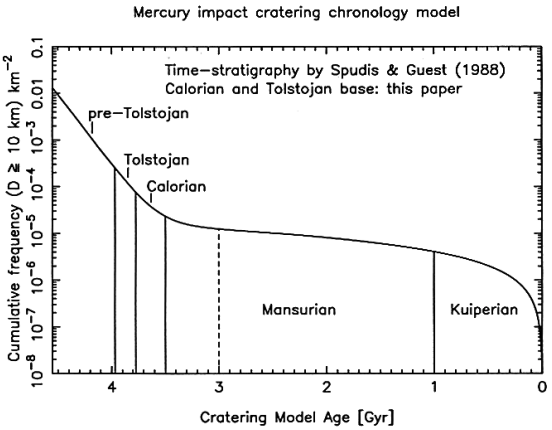

Figure 1: Mercury's impact cratering chronology model and time-stratigraphic system [1, 4]. Age boundaries for Mansurian and Kuiperian periods based on age estimations [4] (*Tab. 1*). Lower boundaries for Tolstojan and Calorian periods from crater size-frequency measurements by [8], with application of the refined production function and the corresponding cratering model ages from the model function discussed in [1].